European Journal of Orthodontics 30 (2008) 190–198
doi:10.1093/ejo/cjm112
Advance Access publication 8 February 2008

The Eulerian buckling test for orthodontic wires

R. De Santis*, F. Dolci**, A. Laino***, R. Martina***, L. Ambrosio* and L. Nicolais*
*IMCB-CNR Institute of Composite and Biomedical Materials, National Research Council, Naples, **Unità Operativa di Ortognatodonzia, PTV Azienda Ospedaliera Universitaria, Policlinico Torvergata, Rome, and ***Department of Odontostomatological and Maxillo-Facial Science, University of Naples "Federico II", Italy

SUMMARY Orthodontic treatment is mainly dependent on the loads developed by metal wires. The load developed by a buckled orthodontic wire is of great concern for molar distalization and cannot be simply derived from mechanical properties measured through classical tests (i.e. tensile, torsion, and bending). A novel testing method, based on the Eulerian approach of a simple supported beam, has been developed in order to measure the load due to buckling of orthodontic wires. Elastic titanium molybdenum alloy (TMA; SDS Ormco) and superelastic Nitinol (3M Unitek) and copper nickel–titanium (NiTi; SDS Ormco) wires, each having a rectangular cross section of 0.016 × 0.022 square inches (0.41 × 0.56 mm^2), were used. The wires were activated and deactivated by loading and unloading. In order to analyse thermo-mechanical properties in buckling, mechanical tests were assisted by calorimetric measurements through differential scanning calorimetry (DSC). Statistical analysis to determine differences between the samples was undertaken using two-way analysis of variance (ANOVA) and Tukey's *post hoc* test, and one-way ANOVA to assess differences between the tested wires under similar conditions and different materials.

The results suggest that the load due to buckling depends on material composition, wire length, the amount of activation, temperature, and deformation rate. The results can be considered as the lower bound for the loads experienced by teeth as far as a buckled wire is concerned. At a temperature higher than the austenite finish transition temperature, superelastic wires were strongly dependent on temperature and deformation rate. The effect due to an increase of deformation rate was similar to that of a decrease of temperature. Load variations due to temperature of a superelastic wire with a length of 20 mm were estimated to be approximately 4 g/°C. The high performance of an applied superelastic wire may be related to the high dynamics of the load in relation to temperature.

Introduction

The force developed by a deformed wire is transmitted to the teeth through fixed appliances (e.g. brackets, molar bands, and tubes) and tooth movements are achieved. Therefore, the load generated by orthodontic wires is of importance in designing an appropriate treatment plan.

As reported by Andreasen and Hilleman (1971), a nickel–titanium (NiTi) based alloy, Nitinol, was first used for orthodontic applications at the beginning of 1960. This alloy contained 55 per cent nickel and 43 per cent titanium, with a stoichiometric balance of 1:1. Further research was then undertaken to assess the orthodontic capability of this material (Andreasen *et al.*, 1985; Harris *et al.*, 1988).

A new titanium alloy for orthodontic applications comprising 11 per cent molybdenum, 6 per cent zirconium, and 4 per cent beta titanium was proposed by Burstone and Goldberg (1980). By tempering this alloy, an orthodontic wire is obtained with a combination of adequate spring back and low rigidity (Kusy and Greenberg, 1982). The elastic modulus of beta titanium is almost double that of Nitinol and half that of stainless steel (Wen *et al.*, 1997).

However, these wires behave as elastic materials; therefore, the developed load drops drastically as the movement of teeth is achieved. A variety of wires based on the superelastic feature of NiTi alloy are available (Ingram *et al.*, 1986; Yoneyama *et al.*, 1992; Wen *et al.*, 1997). Clinical trials clearly show the higher performance of superelastic compared with steel wires (Weiland, 2003). Superelastic alloys are nowadays common engineering materials adopted for several medical applications (Duerig *et al.*, 1996; Thompson, 2000; Kusy, 2002). These materials take advantage of the elastic and thermal deployment, kink resistance, constant unloading stress, and biomechanical and magnetic resonance compatibility (Ingram *et al.*, 1986).

Since the properties of superelastic wires are strongly dependent on temperature (Tonner and Waters, 1994; Sakima *et al.*, 2006), differential scanning calorimetry (DSC) has been used to investigate temperature transition (Bradley *et al.*, 1996; Barwart *et al.*, 1999; Gil and Planell, 1999).

Tensile tests provide a powerful tool to determine the mechanical behaviour of elastic and superelastic wires (van der Wijst *et al.*, 1997; Lammering and Schmidt, 2001; Rucker and Kusy, 2002). Since the properties of superelastic metal alloys depend on the testing mode, mechanical experiments have been also performed by cycling between the tension and the compression modes (Liu *et al.*, 1999; Favier *et al.*, 2002). However, in orthodontic applications, a wire is not

purely stretched or compressed. Torsion tests have also been employed in order to determine mechanical properties of wires (Filleul, 1989; Meling and Odegaard, 1998; Torrisi, 1999). Bending tests represent the easiest way to characterise a wire by providing the load necessary to deflect a wire for a given amount according to the cantilever (Burstone *et al.*, 1985) and three-point bending (Wilkinson *et al.*, 2002; Johnson, 2003) configurations. The simplicity of the bending test set-up has also favoured the evaluation of temperature dependence properties (Tonner and Waters, 1994; Sakima *et al.*, 2006).

Unfortunately, mechanical data based on classical tensile, torsion, and bending do not directly provide the load due to buckling that a wire is capable of transferring to teeth (Nikolai and Chung, 1999; Raboud *et al.*, 2000). Therefore, data based on tensile, torsion, and bending loads developed by orthodontic wires are important from an engineering point of view, but less useful in clinical practice involving buckling force.

An applied orthodontic wire releases the stored elastic energy to the teeth by transmitting loads and torques (Rudolph *et al.*, 2001). Often, the wire is intentionally deformed (e.g. bent or buckled) and joined to fixed appliances (e.g. brackets, molar bands, and tubes) in order to treat Class II malocclusions (Locatelli *et al.*, 1992; Kalra, 1995; Giancotti and Cozza, 1998; Akin *et al.*, 2006). These clinical reports suggest that the main force component generated by the wire for distalizing molars is the load due to buckling (Nikolai and Chung, 1999). This force can be determined using the buckling approach and mechanical protocols for testing straight wires differ for the constraint conditions used at the ends of the wire (Gere and Timoshenko, 1997). The fixed-end conditions produce constraints on orthodontic wires that exceed those of the clinical setting (Nikolai and Chung, 1999). Therefore, loads due to buckling measured through fixed-end conditions can be considered as an upper bound for the loads experienced by teeth during clinical applications.

The aim of this investigation was to assess the mechanical behaviour of elastic and superelastic orthodontic wires using a novel test based on the Eulerian buckling test of a uniform column, simply supported at its ends.

Materials and methods

Elastic titanium molybdenum alloy (TMA; SDS Ormco, Glendora, California, USA), Nitinol (3M Unitek, St Paul, Minnesota, USA), and copper NiTi (CuNiTi; SDS Ormco) wires, each having a rectangular cross section of 0.016 × 0.022 square inches (0.41 × 0.56 mm^2), were used.

DSC was carried out in order to determine the temperature transitions of these wires using the scanning calorimeter Q1000 (TA Instruments Waters LLC, New Castle, Delaware, USA). Specimens (average weight 6.5 ± 0.5 mg) were subjected to heating and cooling cycles between −20 and 50°C at a rate of 10°C/minute. Five specimens for each type of wire were used.

Mechanical testing was performed according to the Euler buckling test. The experiments were carried out using the in-house-designed test fixtures which allow for wire rotation around the pivot points of each hinge (Figure 1). Buckling is generated along the short side of the cross-section of the

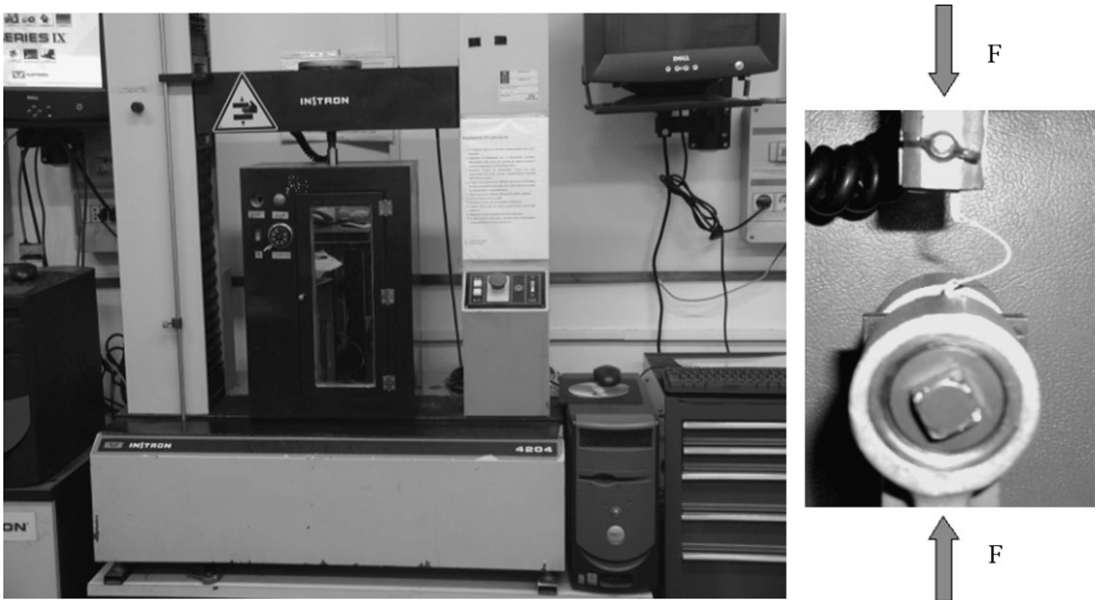

Figure 1 Thermo-mechanical set-up showing the computer-controlled dynamometer and the thermal chamber used to deform orthodontic wires. The photograph on the right shows the detail of the buckling test according to the Eulerian approach. The force monitored by the loading cell (*F*) represents the load due to buckling.

wire. Compared with the fixed-end protocol (Nikolai and Chung, 1999), this set-up configuration is known as the simply supported buckling test.

Each extremity of the wire was crimped in an aluminium tube using a miniature Invecta cutter ODG-1021 (GAC Instruments Inc., Central Islip, New York, USA), adjusted with a stop screw to prevent damage. The tube was fixed through a cylindrical hinge to the chuck of the Instron 4204 dynamometer (High Wycombe, Bucks, UK). Figure 1 shows the thermo-mechanical set-up used to deform orthodontic wires during buckling, consisting of a computer-controlled dynamometer equipped with a thermal chamber. According to the Eulerian approach, the wire was loaded through two parallel and opposite cylindrical hinges; therefore, torque was annulled by these mechanical joints and the force monitored by the loading cell along the axis of the dynamometer represented the buckling load (F).

Straight wires with lengths of 15, 20, 25, and 30 mm were deformed at a speed of 1 mm/minute and at a temperature of 37°C (±1.5°C). One hundred and twenty specimens for each type of wire were used and activated (maximum displacement) at 3, 6, and 9 mm. A load cell of 100 N was used for the wires of 15 mm, and a load cell of 10 N for wires with a length greater than 15 mm. Statistical differences among the samples were assessed using two-way analysis of variance (ANOVA) and the Tukey's *post hoc* test.

In order to investigate the effect of temperature on buckling behaviour, wires with a length of 20 mm underwent an activation of 6 mm. Fifty specimens for each type of wire were divided into five samples according to temperature condition (24, 30, 37, 43, and 50°C). The Fluke 51-2 digital thermometer (Fluke Corp., Everett, Washington, USA) was used to monitor temperature.

The effect of deformation rate on the buckling behaviour was investigated using wires with a length of 20 mm at 37°C (±1.5°C). Thirty specimens of each type of wire were characterized at a speed of 1, 10, and 100 mm/minute.

One-way ANOVA was used to assess statistical differences between wires tested under similar conditions and using differing types of material. This analysis was also used to investigate the effect of temperature on calorimetric and mechanical measurements, and the effect of speed on mechanical properties.

Results

Figure 2 shows the DSC profiles of the investigated orthodontic wires. Endothermic and exothermic processes on heating and cooling were evident for the Nitinol and CuNiTi wires. Therefore, these materials undergo a transition; a martensite–austenite transition was observed upon heating, while the reverse transition was detected on cooling. For TMA, a flat profile was observed, suggesting that this material does not undergo transition, at least in the investigated temperature range.

Different start and finish transition temperatures were found for both Nitinol and CuNiTi wires and a higher specific heat on heating and cooling was measured for the CuNiTi sample (Table 1). On heating, the austenite finish (Af) temperature of both Nitinol and CuNiTi wires was lower than body temperature, suggesting that once these wires are applied, their state is austenitic. The Af temperature of CuNiTi was higher than that of NiTi ($P < 0.01$). On cooling, the martensite start (Ms) and finish (Mf) temperatures of CuNiTi wires were lower than the Nitinol specimens ($P < 0.01$). Moreover, the specific heat measured for CuNiTi was higher than that of Nitinol ($P < 0.01$).

The mechanical behaviour in buckling at 37°C of TMA, NiTi, and CuNiTi wires, with a length of 15 mm and activated up to 3, 6, and 9 mm, are shown in Figure 3. Each load–displacement curve forms a hysteresis loop. A loop consists of loading and unloading steps representing the activation and deactivation phases. The activation phase of wires can be divided into two segments: a pre- and post-buckling activation (Nikolai and Chung, 1999). The end point of the steep slope which characterises the pre-buckling activation phase provides the critical load at which buckling occurs. However, data related to these measurements were widely scattered, preventing the statistical determination of the critical load between wires of the same length.

The post-buckling activation phase can be divided into two segments. The first is a steep decreasing slope, and the second depends on the type and length of the wire. The profile of this segment was a decreasing slope for TMA with a length of 15 mm (Figure 3a). However, as the length of this wire was increased, the slope changed and an increasing slope was observed for TMA with a length of 30 mm. Decreasing profiles were instead always observed for NiTi

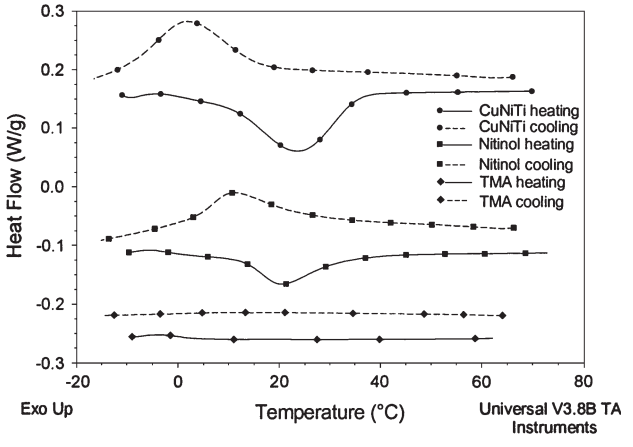

Figure 2 Differential scanning calorimetry profiles of the investigated orthodontic wires. Endothermic and exothermic processes on heating (solid lines) and cooling (dashed lines) are evident for Nitinol and copper NiTi (nickel–titanium) wires. These materials undergo phase transition; martensite–austenite transition is observed on heating, while the reverse transition occurs on cooling.

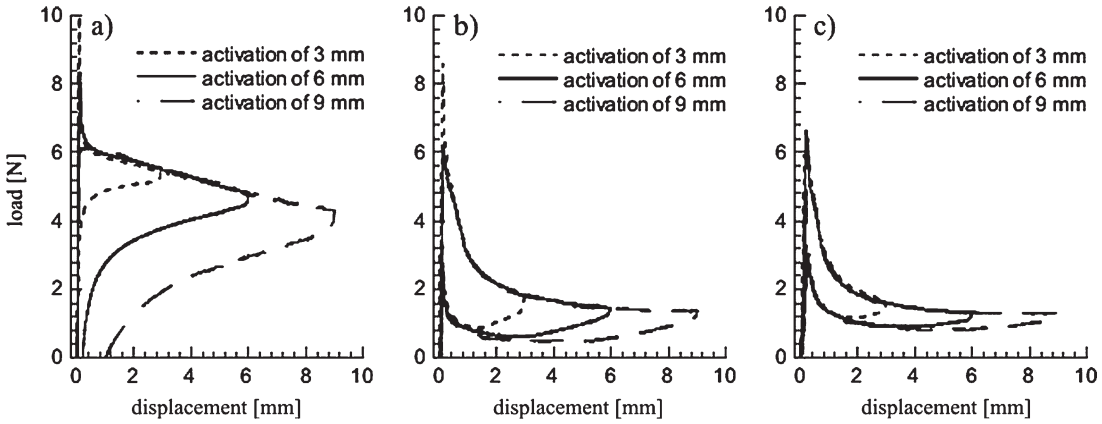

Figure 3 Mechanical behaviour in buckling of TMA (a), Nitinol (b), and copper NiTi (c) with a length of 15 mm at 37°C according to the amount of activation. The pre- and post-buckling activation and the post-buckling and unbuckled deactivation segments (Nikolai and Chung, 1999) can be distinguished.

Table 1 Calorimetric properties of the investigated wires. As, Af, Ms, and Mf denote the austenite start and finish temperatures and the martensite start and finish temperatures, respectively. Endothermic and exothermic specific heat on heating and cooling are indicated with a negative or positive sign, respectively. Each number represents the average value obtained over five measurements. Numbers in brackets represent standard deviations.

	Heating			Cooling		
	As (°C)	Af (°C)	Heat (J/g)	Ms (°C)	Mf (°C)	Heat (J/g)
TMA	—	—	—	—	—	—
Nitinol	13.5 (0.5)	32.3 (0.9)	–4.5 (0.7)	26.2 (0.9)	–3.2 (0.3)	3.9 (0.6)
Copper NiTi	11.3 (0.6)	35.6 (0.7)	–10.4 (1.9)	16.0 (0.6)	–8.7 (0.4)	8.3 (1.3)

and CuNiTi wires (Figure 3b,c), suggesting that these materials undergo austenite–martensite transition.

The start force during the deactivation phase depends on the type, the length, and the maximum deformation of the wire. Higher values were measured for TMA. The start force value for NiTi and CuNiTi wires decreased as the length of the wire or the maximum deformation was increased. Table 2 shows the magnitude of this load measured at 37°C, and the results of the two-way ANOVA are reported in Table 3. TMA provided force values higher than NiTi and CuNiTi ($P < 0.01$) for every wire length and for each activation. The start deactivation force of NiTi wires with a length of 15 and 20 mm was higher than the corresponding CuNiTi values ($P < 0.01$) but only for an activation of 3 mm. A weaker statistical difference ($P < 0.05$) was observed between NiTi and CuNiTi wires with a length greater than 20 mm or activated at 6 and 9 mm. For each type of wire, the statistical significance of the main effects (wire length and activation amount) and of the interaction (length × activation) can be deduced from Table 3. The F value represents the ratio of the variance from the particular source effect relative to error variance. For each type of wire, both the length and activation provided $F > 1$ and significance level of $P < 0.01$; therefore, these effects are significant. For each type of wire, Tukey's *post hoc* test suggests that the mean difference was significant at the 0.01 level for both wire length and activation amount.

The results shown in Table 3 suggest that TMA is very sensitive to the length of the wire while NiTi and CuNiTi are very sensitive to the amount of activation. These results are consistent with the profiles of the loads due to buckling as a function of the activation amount (Figure 3). The significant interaction effect observed for TMA (Table 3) indicates that the differences between the wire length depend on the amout of activation. The force value of TMA activated at 3 mm was higher than that measured after 6 mm activation ($P < 0.01$) but only for lengths of 15 and 20 mm. An inverse trend of the force versus activation amount was observed for TMA wires with a length of 25 and 30 mm. The F value and the significance level of the interaction effect observed for NiTi (Table 3) suggest that wire length differences did not depend on the level of activation amount. For all wire lengths, the force measured for NiTi (Figure 3 and Table 2) activated at 3 mm was higher than that measured after 6 mm of activation ($P < 0.01$). Similar

Table 2 Loads due to buckling (expressed in N) measured at 37°C according to the length and activation. Each number represents the average value obtained over 10 measurements.

	15 mm length			20 mm length			25 mm length			30 mm length		
	Activation			Activation			Activation			Activation		
	3	6	9	3	6	9	3	6	9	3	6	9
TMA	5.49	4.79	4.28	4.09	3.88	3.60	2.46	2.51	2.55	1.83	1.85	1.88
NiTi	1.89	1.45	1.36	1.75	1.32	1.21	1.49	1.09	0.94	1.37	0.99	0.83
Copper NiTi	1.63	1.32	1.28	1.42	1.11	1.02	1.28	0.94	0.78	1.19	0.89	0.75

Table 3 Two-way analysis of variance results. The start force is the dependent variable while the wire length and the amount of activation are the independent variables. The length × activation values provide the interaction effect of the wire length and activation amount.

Wire	Source	Type III sum of squares	Degrees of freedom	Mean square	*F* value	Significance level
TMA	Wire length	163.3	3	54.42	2201	0.000
	Activation	2.925	2	1.462	59.15	0.000
	Length × activation	5.544	6	0.924	37.38	0.000
NiTi	Wire length	4.854	3	1.618	219.9	0.000
	Activation	6.449	2	3.225	438.3	0.000
	Length × activation	0.021	6	0.004	0.484	0.819
Copper NiTi	Wire length	4.015	3	1.338	684.2	0.000
	Activation	3.860	2	1.930	986.5	0.000
	Length × activation	0.070	6	0.012	5.933	0.000

results were found for CuNiTi wire and a weak interaction effect was observed (Table 3).

Figure 3 shows that the profile of the deactivation phase depends on the material. TMA (Figure 3a) showed the typical behaviour of elastic materials which undergo plastic deformation during the activation phase. The load dropped to zero following a steep slope. For TMA wires with a length of 15 mm activated at 9 mm, a maximum permanent deformation of 1 mm was measured. Different deactivation profiles were observed for superelastic wires (Figure 4b,c). The deactivation phase of NiTi and CuNiTi wires can be divided into two segments: post-buckling deactivation and unbuckled deactivation (Nikolai and Chung, 1999). A minimum in the post-buckling deactivation segment was evident for superelastic wires, suggesting that the martensite–austenite transition was occurring. This transition is stress driven and the plateau in the post-buckling deactivation segment represents the ability of the orthodontic wire to apply a load to the bonded teeth at a fairly constant value over a wide range of deformation.

The effect of temperature on the deactivation phase is shown in Figure 4. The behaviour of TMA (Figure 4a) was independent of temperature, while a strong dependence was observed for NiTi and CuNiTi (Figure 4b,c). At room temperature, during unloading, the buckling load developed by the superelastic wires was fairly low and a plastic deformation of each wire was observed as the load approached zero (Figure 4b,c). This plastic deformation can be ascribed to the martensite phase. In fact, room temperature is below Af temperatures of both Nitinol and CuNiTi (Figure 2, Table 1). Therefore, at a temperature below Af, after removal of the buckling load, only a partial recovery of the deformation was observed. However, different behaviour was noted when testing at temperatures above Af (e.g. body temperature). Figure 4b,c shows that NiTi and CuNiTi recovered the whole deformation as the buckling load was removed at 37°C. Therefore, on unloading, complete transition to the austenitic phase was achieved.

The deactivation start force for both NiTi and CuNiTi measured at 50°C was higher than that measured at 37°C ($P < 0.01$). For both superelastic wires, an increase of approximately 1 N was measured in post-buckling deactivation (Figure 4b,c) as the temperature was raised from 24 to 50°C. Therefore, the effect of temperature on the load developed by NiTi and CuNiTi wires with a length of 20 mm is approximately 4 g/°C. Figure 4b,c also shows that the minimum value in the post-buckling deactivation segment shifted to higher displacement values as the temperature was increased, suggesting that this minimum depends on the martensite–austenite transition.

Figure 5 shows the effect of the deformation rate on the deactivation phase at 37°C. The behaviour of TMA

(Figure 5a) was independent of deformation rate, while a marked dependence on the deformation rate was observed for NiTi and CuNiTi (Figure 5b,c). The deactivation start force of NiTi measured at 100 mm/minute was higher than that measured at 1 mm/minute ($P < 0.01$). The minimum value in the post-buckling deactivation segment shifted to a higher displacement level as the deformation rate decreased. The peak value, which divides the post-buckling and the unbuckled deactivation segments, shifted to a higher load as the deformation rate was decreased. Similar results were observed for CuNiTi (Figure 5c). Comparison of Figures 4b,c and 5b,c demonstrates that the effect due to an increase in temperature was comparable with the effect resulting from a decrease in the deformation rate.

Discussion

An applied orthodontic wire releases the stored elastic energy to the teeth by transmitting loads and torques (Rudolph *et al.*, 2001). A wire deformed similar to that shown in Figure 1 is often used to treat Class II malocclusions (Locatelli *et al.*, 1992; Kalra, 1995; Giancotti and Cozza, 1998; Akin *et al.*, 2006). The deformation of a wire achieved through buckling is similar to that obtained through a standard bending test. However, the transverse load measured using the standard three-point bending test is different from that measured with the buckling test (Nikolai and Chung, 1999). The load due to buckling (Figure 1) is more appropriate to describe the load involved in molar distalization.

Proportionality between the applied load and deflection was observed for wires tested in bending using a span of 14 mm (Garrec *et al.*, 2005). Figure 3 shows that in the post-buckling activation, the loads of wires with a length of 15 mm were inversely proportional to the amount of activation. This load decrease was also related to a reduction of the elastic modulus for superelastic wires since a phase transition occurs (Figure 3b,c). However, a decreasing trend

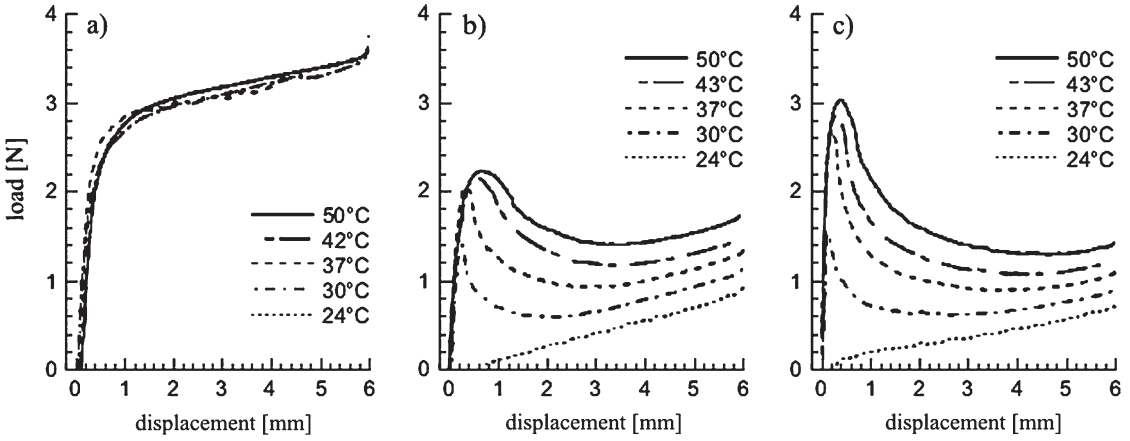

Figure 4 Temperature dependence of the load during deactivation of TMA (a), Nitinol (b), and copper NiTi (c) with a length of 20 mm. Loads due to buckling of superelastic wires increase at a rate of approximately 4 g/°C. This temperature dependence confers high dynamics to superelastic wires.

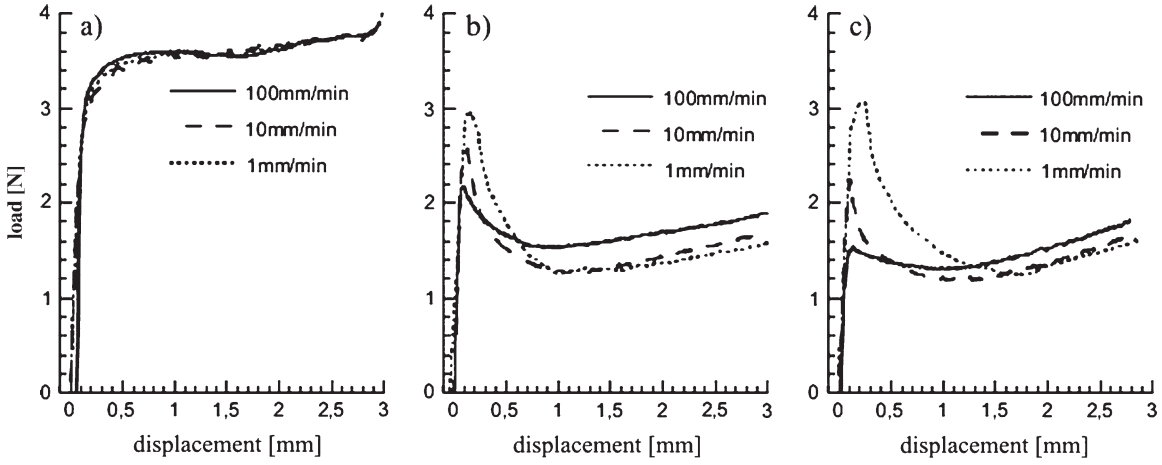

Figure 5 Deformation rate dependence of the load during deactivation of TMA (a), Nitinol (b), and copper NiTi (c) with a length of 20 mm. Loads due to buckling of superelastic wires increase as deformation is decreased.

in the post-buckling deactivation segment was evident for the elastic TMA (Figure 3a). Interestingly, this trend changed as the wire length was increased (Table 2). Therefore, forces measured through bending are different from those measured through buckling, also from a qualitative point of view.

Proportionality between the applied load and stiffness has been detected through tensile (Rucker and Kusy, 2002), torsion (Filleul, 1989), and bending (Garrec *et al.*, 2005) tests. This result is similar for buckling tests through both the simply supported configuration (Figure 3, Table 2) and the fixed-ends configuration (Nikolai and Chung, 1999). Stiffness is the product between the elastic modulus and a geometric property (e.g. the second moment of area). Therefore, both Young's modulus (type of wire) and the thickness of the wire can be conveniently chosen in order to tailor the load for the specific treatment plan. In the present experiments, wires with similar dimensions were used; thus, wire stiffness differs only for Young's modulus. Figure 3 shows that the critical load which induces buckling (the peak in the activation phase, which separates the unbuckling from the buckling segment) is reduced by approximately one-third for superelastic wires, which is consistent with stiffness measurements of beta titanium and austenitic NiTi (Burstone and Goldberg, 1980; Rucker and Kusy, 2002; Johnson, 2003; Garrec *et al.*, 2005). The slight difference between NiTi and CuNiTi in the critical load due to buckling (Figure 3b,c) can be related to the lower stiffness measured for CuNiTi (Wilkinson *et al.*, 2002). The decrease of the load observed for NiTi and CuNiTi as the amount of activation is increased (Figure 3, Table 2) can be related to the decrease in Young's modulus due to phase transformation (Garrec *et al.*, 2005). These results clearly indicate that wire length and the amount of activation represent a powerful tool for calibrating the load in clinical trials. Elastic TMA is very sensitive to the length of the wire, while superelastic wires are very sensitive to the amount of activation (Table 3).

The effects of temperature on the load due to buckling (Figure 4) are consistent, from a qualitative point of view, with the results obtained through bending tests (Wilkinson *et al.*, 2002). The load values for TMA (Figure 4a) showed little variation as the temperature was increased or decreased, while NiTi and CuNiTi (Figure 4b,c) were very sensitive to temperature. An increase of approximately 1 N was measured as the temperature was increased from 24 to 50°C; thus, the effect of temperature can be estimated to be approximately 4 g/°C for a wire with a length of 20 mm. The temperature of an archwire over a daily period is reported to be between 33 and 37°C for 79 per cent of this period (Moore *et al.*, 1999). Although this temperature range is low, the effect on the load variation developed by superelastic wires is expected to be about 15 per cent. A more significant effect of temperature on the load developed by wires is expected for the remaining 21 per cent of a daily period. Figure 4 shows that load variation of superelastic wires can be as high as 100 per cent, which is consistent with bending tests results (Wilkinson *et al.*, 2002). It is difficult to determine the clinical implications of load variation due to temperature of an applied superelastic wire. It is reported that teeth activated with superelastic wires move significantly more than teeth moved with steel wires (Weiland, 2003). The reason for the higher performance of superelastic wires is generally ascribed to the fairly constant value over a wide range of deformation (Duerig *et al.*, 1996; Auricchio *et al.*, 2004) in contrast to the load decrease generally observed for other type of wires (Figure 3). However, temperature effects are insignificant (Figure 4) and it is incorrect to state that the load developed by applied superelastic wires is almost constant. On the other hand, mechanisms for bone adaptation involve a process of cellular mechanotransduction driven by dynamic rather than static loading (Turner and Pavalko, 1998; Gross *et al.*, 2002). Therefore, the higher performance of superelastic wire may be related to the pronounced dynamics of the load in relation to temperature variations.

Superelastic wires are also sensitive to deformation rate (Figure 5b,c). The effect on the load due to an increase of deformation rate is similar to the effect due to a decrease of temperature (Figure 4b,c). This is important from an engineering point of view, suggesting a simplification of mechanical models of superelastic wires in the time–temperature domain. The deformation rate of an applied orthodontic wire is very slow compared with those used *in vitro*. Thus, deactivation loads measured through mechanical tests may underestimate the loads experienced by teeth.

From a qualitative point of view, the results obtained by measuring loads due to buckling at 37°C using the simply supported condition (Figure 3, Table 2) corroborate the findings of Nikolai and Chung (1999) measured through the fixed-end condition. From a quantitative point of view, load measurements using the fixed-end condition can be considered as an upper bound for the loads produced by wires in a clinical setting. The results obtained through the simply supported condition represent a lower bound for the loads experienced by teeth in clinical trials.

Conclusions

Following the Eulerian approach, a novel method is introduced to accurately measure the buckling load developed by orthodontic wires. The results of this study show the following.

1. TMA develops a higher force than NiTi and CuNiTi wires but this force drops to zero during unloading following a steep slope.
2. At 37°C and upon unloading, the superelastic feature of NiTi and CuNiTi is manifested through a fairly constant value of the load over a wide range of deformation.
3. For superelastic wires, the load due to buckling decreases as the wire length or the amount of activation is increased.

4. At body temperature, the start force level on deactivation of NiTi wires is slightly higher than that of CuNiTi wires, thus suggesting that copper softens the alloy structure.
5. The load due to buckling of superelastic wires is temperature and time dependent (i.e. strain rate dependent). The effect on the load due to an increase of deformation rate is similar to the effect due to a decrease of temperature.
6. Load variation of superelastic wires due to temperature change in the oral environment may support the hypothesis that the high performance of superelastic wires is related to the high dynamics of these wires.
7. Loads measured through the simply supported condition and those measured through the fixed-end condition can be considered as a lower and upper bound for the load developed by a wire in a clinical setting.

Address for correspondence

Roberto De Santis
IMCB-CNR
Institute for Composite and Biomedical Materials
National Research Council
Piazzale Tecchio 80
Naples 80125
Italy
E-mail: rosantis@unina.it

Funding

CRdC of Regione Campania, Work Package 1C 'Innovazione nelle tecnologie dei biomateriali e ricostruzione dei tessuti' (POR 2006 regione campania, misura 3.16).

Acknowledgements

The authors also wish to thank Dr Antonio Giliberti and Mr Rodolfo Morra for the mechanical testing and Dr Francesco Mollica for useful discussions.

References

Akin E, Gurton A U, Sagdic D 2006 Effects of a segmented removable appliance in molar distalization. European Journal of Orthodontics 28: 65–73

Andreasen G F, Hilleman T B 1971 An evaluation of 55 cobalt substituted nitinol wire for use in orthodontics. Journal of the American Dental Association 82: 1373–1375

Andreasen G, Wass K, Chan K C 1985 A review of superelastic and thermodynamic nitinol wire. Quintessence International 16: 623–626

Auricchio F A, Cacciafesta V C, Petrini L P, Pietrabissa R P 2004 . On the mechanics of super elastic orthodontic appliances. In: Natali A N (ed). Dental biomechanics Taylor and Francis, London, pp. 132–158.

Barwart O, Rollinger J M, Burger A 1999 An evaluation of the transition temperature range of superelastic orthodontic NiTi springs using differential scanning calorimetry. European Journal of Orthodontics 21: 497–502

Bradley T G, Brantley W A, Culbertson B M 1996 Differential scanning calorimetry (DSC) analyses of superelastic and nonsuperelastic nickel-titanium orthodontic wires. American Journal of Orthodontics and Dentofacial Orthopedics 109: 589–597

Burstone C J, Goldberg A J 1980 Beta-titanium: a new orthodontic alloy. American Journal of Orthodontics 77: 121–132

Burstone C J, Qin B, Morton J Y 1985 Chinese NiTi wire—a new orthodontic alloy. American Journal of Orthodontics 87: 445–452

Duerig T W, Pelton A R, Stokel D, Wayman C M 1996 The utility of superelasticity in medicine. Biomedical Materials and Engineering 6: 255–266

Favier D, Liu Y, Orgeas L, Rio G 2002 Mechanical instability of NiTi in tension, compression and shear. In: Sun Q P (ed.), IUTAM symposium on micromechanics of martensitic phase transformation in solids. Kluwer Academic Publishers, Dordrecht, pp. 205–212

Filleul M P 1989 A comparison of archwires of memory alloys Nitinol, NiTi Ormco and Tru-chrome which were subjected to edgewise torsion of 20 degrees, 25 degrees, 30 degrees and 35 degrees and a temperature of 37 degrees Celsius. L'Orthodontie Francaise 60: 851–860

Garrec P, Tavernier B, Jordan L 2005 Evolution of flexural rigidity according to the cross-sectional dimension of a superelastic nickel titanium orthodontic wire. European Journal of Orthodontics 27: 402–407

Gere J M, Timoshenko S P 1997 Buckling. In: Mechanics of materials. 4th edn. PWS Publishing Company, Boston, pp. 731–804.

Giancotti A, Cozza P 1998 Nickel titanium double-loop system for simultaneous distalization of first and second molars. Journal of Clinical Orthodontics 32: 255–260

Gil F J, Planell J A 1999 Effect of copper addition on the superelastic behavior of Ni-Ti shape memory alloys for orthodontic applications. Journal of Biomedical Materials Research 48: 682–688

Gross T S, Srinivasan S, Liu C C, Clemens T L 2002 Noninvasive loading of the murine tibia: an *in vivo* model for the study of mechanotransduction. Journal of Bone and Mineral Research 17: 493–501

Harris E F, Newman S M, Nicholson J A 1988 Nitinol arch wire in a simulated oral environment: changes in mechanical properties. American Journal of Orthodontics and Dentofacial Orthopedics 93: 508–513

Ingram Jr S B, Gipe D B, Smith R J 1986 Comparative range of orthodontic wires. American Journal of Orthodontics and Dentofacial Orthopedics 90: 296–307

Johnson E 2003 Relative stiffness of beta titanium archwires. Angle Orthodontist 73: 259–269

Kalra V 1995 The K-loop molar distalizing appliance. Journal of Clinical Orthodontics 29: 298–301

Kusy R P 2002 Orthodontic biomaterials: from the past to the present. Angle Orthodontist 72: 501–512

Kusy R P, Greenberg A R 1982 Comparison of the elastic properties of nickel-titanium and beta-titanium arch wires. American Journal of Orthodontics 82: 199–205

Lammering R, Schmidt I 2001 Experimental investigations on the damping capacity of NiTi components. Smart Materials and Structures 10: 853–859

Liu Y, Xie Z, Van Humbeeck J 1999 Cyclic deformation of NiTi shape memory alloys. Materials Science and Engineering 273: 673–678

Locatelli R, Bednar J, Dietz V S, Gianelly A A 1992 Molar distalization with superelastic NiTi wire. Journal of Clinical Orthodontics 26: 277–279

Meling T R, Odegaard J 1998 The effect of temperature on the elastic responses to longitudinal torsion of rectangular nickel titanium archwires. Angle Orthodontist 68: 357–368

Moore R J, Watts J T, Hood J A, Burritt D J 1999 Intra-oral temperature variation over 24 hours. European Journal of Orthodontics 21: 249–261

Nikolai R J, Chung A Y 1999 Controlled localized buckling responses of orthodontic arch wires. American Journal of Orthodontics and Dentofacial Orthopedics 116: 308–316

Raboud D W, Faulkner M G, Lipsett A W 2000 Superelastic response of NiTi shape memory alloy wires for orthodontic applications. Smart Materials and Structures 9: 684–692

Rucker B K, Kusy R P 2002 Elastic properties of alternative versus single-stranded leveling archwires. American Journal of Orthodontics and Dentofacial Orthopedics 122: 528–541

Rudolph D J, Willes P M G, Sameshima G T 2001 A finite element model of apical force distribution from orthodontic tooth movement. Angle Orthodontist 71: 127–131

Sakima M T, Dalstra M, Melsen B 2006 How does temperature influence the properties of rectangular nickel-titanium wires?. European Journal of Orthodontics 28: 282–291

Thompson S A 2000 An overview of nickel-titanium alloys used in dentistry. International Endodontic Journal 33: 297–310

Tonner R I, Waters N E 1994 The characteristics of superelastic Ni-Ti wires in three-point bending. Part I: the effect of temperature. European Journal of Orthodontics 16: 409–419

Torrisi L 1999 The NiTi superelastic alloy application to the dentistry field. Biomedical Materials and Engineering 9: 39–47

Turner C H, Pavalko F M 1998 Mechanotransduction and functional response of the skeleton to physical stress: the mechanisms and mechanics of bone adaptation. Journal of Orthopaedic Science 3: 346–355

van der Wijst M W M, Schreurs P J G, Veldpaus F E 1997 Application of computed phase transformation power to control shape memory alloy actuators. Smart Materials and Structures 6: 190–198

Weiland F 2003 Constant versus dissipating forces in orthodontics: the effect on initial tooth movement and root resorption. European Journal of Orthodontics 25: 335–342

Wen X, Zhang N, Li X, Cao Z 1997 Electrochemical and histomorphometric evaluation of the Ni-Ti-Cu shape memory alloy. Biomedical Materials and Engineering 7: 1–11

Wilkinson P D, Dysart P S, Hood J A, Herbison G P 2002 Load-deflection characteristics of superelastic nickel-titanium orthodontic wires. American Journal of Orthodontics and Dentofacial Orthopedics 121: 483–495

Yoneyama T, Doi H, Hamanaka H, Okamoto Y, Mogi M, Miura F 1992 Superelasticity and thermal behavior of Ni-TI alloy orthodontic arch wires. Dental Materials Journal 11: 1–10